JPE 17-4-24

https://doi.org/10.6113/JPE.2017.17.4.1097
ISSN(Print): 1598-2092 / ISSN(Online): 2093-4718

Applicable Method for Average Switching Loss Calculation in Power Electronic Converters

Seyyed Abbas Saremi Hasari*, Ahmad Salemnia†, and Mohsen Hamzeh*

*, †Faculty of Electrical Engineering, Shahid Beheshti University, Tehran, Iran

Abstract

Accurate calculation of the conduction and switching losses of a power electronic converter is required to achieve the efficiency of the converter. Such calculation is also useful for computing the junction temperature of the switches. A few models have been developed in the articles for calculating the switching energy losses during switching transitions for the given values of switched voltage and switched current. In this study, these models are comprehensively reviewed and investigated for the first time for ease of comparison among them. These models are used for calculating the average amount of switching power losses. However, some points and details should be considered in utilizing these models when switched current or switched voltage presents time-variant and alternative quantity. Therefore, an applicable technique is proposed in details to use these models under the above-mentioned conditions. A proper switching loss model and the presented technique are used to establish a new and fast method for obtaining the average switching power losses in any type of power electronic converters. The accuracy of the proposed method is evaluated by comprehensive simulation studies and experimental results.

Key words: Analytical loss model, Conduction loss model, Power electronic converter loss, Switching loss model

I. INTRODUCTION

Power electronic converters play an important role in the electric power industry because of their applications, such as integrating the distributed energy units into the grid [1], improving the power quality of the grid [2], and driving the electric motors. Electrical power loss is an important concern of power electronic converters. Converter losses usually involve the power losses of the electromagnetic devices and the power losses of the semiconductor switches. Switch power losses consist of three parts: 1) switching losses, 2) conduction losses, and 3) negligible off-state losses.

The switching losses are dominant losses at high switching frequencies and depend on four factors [3]: 1) switched voltage, 2) switched current, 3) switching frequency, and 4) rising and falling times of the switch voltage and current. The switching losses are more difficult to calculate, in comparison with the conduction losses [4]. The difficulty is attributed to the tiny amount of the turn-on and turn-off transition times, and the estimation of switch waveforms during transition times that needs to provide the accurate model of the switch.

Calculating the conduction and switching losses of a power electronic converter is useful for 1) calculating the junction temperature of the switches for designing the heat sink, and 2) obtaining the efficiency of the converter. Efficiency is an important characteristic of power electronic converters and is thus used as an evaluation criterion for five types of DC/AC converters in [5], for two types of AC/AC converters in [6], and for photovoltaic inverters in [7].

The switching losses of the converters can be calculated by three methods [8], [9]: 1) utilizing experimental switching waveforms acquired from the laboratory prototype, 2) utilizing simulation models obtained by the switch datasheet and its electrical and thermal models, and 3) using analytical models.

Unlike the analytical methods, simulation-based methods require calculating the switching energy losses for all the turn-on and turn-off transitions. Analytical methods can be derived when the output current is sinusoidal. In these methods, the average switching power loss is calculated using some information, such as switch characteristics, output displacement factor, amplitude of the output current, and modulation index. Therefore, simulation-based methods exhibit more computational burden compared to analytical methods. However, simulation-based methods can be implemented for all kinds of converters and output currents.

Manuscript received Oct. 3, 2016; accepted May 8, 2017
Recommended for publication by Associate Editor Hyung-Min Ryu.
†Corresponding Author: a_salemnia@sbu.ac.ir
Tel: +982173932502, Fax: +982177310425, Shahid Beheshti University
*Faculty of Electrical Engineering, Shahid Beheshti University, Iran

TABLE I
SOME OF THE CONVERTERS WHICH HAVE ANALYTICAL MODELS FOR SWITCHING LOSS CALCULATION

Converter type	Corresponding references
Matrix Z-source converter (MZC)	[10]
Very sparse matrix converter (VSMC)	[13], [14]
Conventional matrix converter (CMC)	[14]
Sparse matrix converter (SMC)	[14]
Modular multilevel converter (MMC)	[15], [16]
Two-level converter	[17]
Three-level neutral point clamped converter (NPC)	[17]
Three-level and four-level flying capacitor converter (FC)	[17]
Ladder multilevel converter	[18]

An analytical model for a given power converter is derived using two elements [10]: 1) the conduction and switching loss model for each turn-on and turn-off transitions, and 2) the operating principle of the converter. Some of the converters, which have analytical models for computing switching losses, are listed in Table I.

A few semiconductor manufacturers have provided online or offline software tools (e.g., [11], [12]) for calculating the average losses and junction temperature of power switches using loss calculation models. However, these software tools are applicable only for limited types of converters.

The switching loss calculation models are expressed by mathematical equations such as Equs. (1)-(10). As seen, these models can calculate the switching energy losses during turn-on and turn-off transitions for the given values of switched voltage and switched current. In simulation-based methods, these models are required to calculate the average value of switching power losses. However, using these models for alternative switched current or switched voltage requires additional points and details to be considered. Therefore, an applicable technique is presented in this study in details to use these models under the said conditions. This technique is composed of two main steps. The first step samples the switch voltage and current properly, and the second step generates the appropriate square signals. The average amount of square signals will be equal to the average switching power losses.

The switching loss models are comprehensively reviewed in the following, for ease of selection of an appropriate model.

The switching energy losses of a power switch such as a transistor can be calculated by the following equations [3].

$$E_{sw,off} = \int_{t_{off}} i(t).v(t).dt \quad (1)$$

$$E_{sw,on} = \int_{t_{on}} i(t).v(t).dt \quad (2)$$

In the equations above, $i(t)$ is the current passing through the switch; $v(t)$ is the voltage across the switch; $E_{sw,\mathrm{on}}$ and $E_{sw,\mathrm{off}}$ are the switching energy losses of the switch which are calculated during its turn-on transition time t_{on} and turn-off transition time t_{off}, respectively. The above-mentioned method is limited by its need of a precise model of the switch to accurately estimate the waveforms of the switch voltage and current during turn-on and turn-off transitions. Such a precise model is presented in [8] for SiC MOSFETs but requires bulky calculations and detailed parameters of the transistor. The method is also computationally demanding and time consuming [15]. According to [8] and [9], this drawback occurs owing to the tiny values of the falling and rising times of the transistor current and voltage, thereby resulting in an extremely small simulation step time (approximately in nanosecond range).

The problems above can be resolved by finding appropriate equations as the solutions to the integrals in Equs. (1) and (2), instead of solving the integrals by numerical methods. After solving Equs. (1) and (2) using simplified approximations, an analytical expression is obtained for switching losses of a transistor as Equ. (3) for the resistive load [18], and as Equ. (4) for the inductive load [19].

$$E_{sw,x} = \frac{1}{6}.V_{CC,x}.I_{C,x}.t_x \quad (3)$$

$$E_{sw,x} = \frac{1}{2}.V_{CC,x}.I_{C,x}.t_x \quad (4)$$

In the equations above, "x" can be replaced with "*on*" or "*off*" and indicates that the parameter is related to the turn-on or turn-off transition of the switch. $V_{CC,x}$ is the off-state voltage of the transistor, and $I_{C,x}$ is the on-state current of the transistor. $V_{CC,x}$ and $I_{C,x}$ are switched when the transistor is turned on or off. For the inductive load, transition time t_x depends on the rising and falling times of the switch voltage that are not usually given in the switch datasheets.

Curve fitting methods and experimental loss curves of the switch are usually used to derive appropriate equations for switching loss calculation. Using curve fitting, the dependency of the switching energy loss of an IGBT, $E_{sw,x}$, on the switched voltage $V_{cc,x}$ and switched current $I_{c,x}$ is provided by a fourth degree polynomial in [10] as follows.

$$\begin{aligned} E_{sw,x} &= k_{1,x}V_{CC,x}I_{C,x} + k_{2,x}V_{CC,x}I_{C,x}^2 + k_{3,x}V_{CC,x}^2 \\ &+ k_{4,x}V_{CC,x}^2 I_{C,x} + k_{5,x}V_{CC,x}^2 I_{C,x}^2 \end{aligned} \quad (5)$$

In the equation above, $k_{1,x}$, $k_{2,x}$, …, $k_{5,x}$ are the fitting constants, and "x" can be replaced with "*on*" or "*off*." Such an equation can also be used to calculate the diode turn-off losses. According to [10], a notable feature of Equ. (5) is that, the values of $k_{1,x}$ are much greater than the values of other fitting constants.

In [15], [17], and [20], the switching losses are estimated by Equ. (6) using curve fitting methods. It shows that, the switching losses are related to a quadratic polynomial in the switched current $I_{C,x}$, and are linearly related to the switched voltage $V_{CC,x}$.

$$E_{sw,x} = (a_x I_{C,x}^2 + b_x I_{C,x} + c_x) \times \frac{V_{CC,x}}{V_{CC,x}^*} \quad (6)$$

In the equation above, $V^*_{CC,x}$ is the switched voltage used to acquire the experimental switching loss curves, and "*x*" can be replaced with "*on*" or "*off*." In the said works, the values of the fitting constant a_x, are approximately 10^{-4} to 10^{-3} times smaller than the values of b_x and c_x.

In [5] and [21], the switching losses are expressed as Equ. (7) with a linear relationship to $(I_{C,x})^{B_x}$. In [22], this equation is improved as Equ. (8). This equation shows that, the switching loss is dependent on the switched voltage $V_{CC,x}$ in addition to the switched current $I_{C,x}$.

$$E_{sw,x} = A_x.(I_{C,x})^{B_x} \tag{7}$$

$$E_{sw,x} = A'_x.(I_{C,x})^{B_x}.\frac{V_{CC,x}}{V^*_{CC,x}} \tag{8}$$

In the equations above, A_x, A'_x, and B_x, are the fitting constants and "*x*" can be replaced with "*on*" or "*off*." Switching loss curves are plotted on log-log scales in [23] to obtain the values of the fitting constants in Eq. (7). In the said works, the values of B_x are approximately equal to 1 for IGBTs.

Considering the properties of Equs. (5)–(8), the following conclusions can be obtained. The turn-on and turn-off switching energy losses of the IGBTs present a nearly linear relationship with the switched current and switched voltage as stated in [9]. This linear relationship is clearly demonstrated in [24] and [25] by the following equations.

$$E_{sw,off} = E^*_{sw,off}.\frac{V_{CC,off}}{V^*_{CC,off}}.\frac{I_{C,off}}{I^*_{C,off}} \tag{9}$$

$$E_{sw,on} = E^*_{sw,on}.\frac{V_{CC,on}}{V^*_{CC,on}}.\frac{I_{C,on}}{I^*_{C,on}} \tag{10}$$

In the equations above, $E^*_{sw,on}$ and $E^*_{sw,off}$ are the experimentally measured values for the switching energy losses of the transistor during its turn-on and turn-off transitions, respectively. They are available in the transistor datasheets for the given $V^*_{CC,x}$ and $I^*_{C,x}$. Parameter $V^*_{CC,x}$ is the measured off-state voltage of the transistor, and $I^*_{C,x}$ is the measured on-state current of the transistor. These components are switched during the transition time, so can be named switched voltage and switched current. $E_{sw,on}$ and $E_{sw,off}$ are the switching energy losses of the transistor during its turn-on and turn-off transitions, respectively. They are calculated for the intended switched off-state voltage V_{CC}, and switched on-state current I_C.

The switching losses vary depending on the gate impedance, parasitic circuit elements [8], and snubber characteristics. However, this linear approximation provides a good accuracy, particularly near the test point of the manufacturer ($V^*_{CC,x}$ and $I^*_{C,x}$) and the snubber condition [4], [25].

As a valuable feature of this study, the switching loss models were comprehensively reviewed in Section I, to ease the selection of the appropriate loss model. This paper mainly contributes by establishing an applicable technique in details for calculating the average value of switching power losses using switching loss models. This technique can be utilized in any type of converters, and has the following advantages. 1) This technique is useful for alternative switched current or switched voltage. 2) This technique can be implemented easily using the basic blocks of programs such as MATLAB/SIMULINK. 3) The proposed technique samples the switched voltage and current properly. 4) This technique uses a simple and creative approach for saving and averaging the switching losses.

In the following sections of the paper, the proposed method for obtaining the average value of switching power losses is described first. Then, the conduction loss models for calculating the total losses of the converter are investigated. Finally, the accuracy of the proposed method is evaluated by simulation and experimental results.

II. New Method for Calculating Average Switching Power Losses

In this section, a new method for calculating the average switching power losses of a transistor with an antiparallel diode is proposed and described in detail. In the proposed method, switch losses are considered without dependency on the junction temperature. This method is composed of three parts: 1) selecting a proper switching loss model, 2) sampling the switch voltage and current correctly, and 3) generating appropriate square signals. These parts are described below.

Using Equs. (1) and (2) for calculating switching losses is computationally demanding, time consuming, and requires a precise model of the switches. As stated previously, these drawbacks can be overcome by utilizing curve-fitting methods to obtain switching loss models. Therefore, in the current study, Equs. (9) and (10) are selected as switching-loss calculation models because of their less computational burden. Moreover, the parameter values of these models are easily obtained via the transistor datasheets.

The average amount of switching power losses of a switch $\overline{P_{sw}}$, can be calculated as Equ. (11) by considering constant amounts for $V_{CC,x}$ and $I_{C,x}$ in Equs. (9) and (10). In this equation, f_{sw} is the switching frequency. Such a condition can occur in the DC–DC converters.

$$\overline{P_{sw}} = f_{sw}.\left(E_{sw,on} + E_{sw,off}\right) \tag{11}$$

However, Equ. (11) is inapplicable for an inverter because of the variable and periodic feature of $I_{C,x}$ in each switch of the inverter [23]. $I_{C,x}$ in Equs. (9) and (10) is substituted with the absolute average value of switch current $|I_{ave}|$ in [16] to solve the said problem. Therefore, Equ. (11) is modified as

$$\overline{P_{sw}} = \left(E^*_{sw,on} + E^*_{sw,off}\right).\frac{V_{CC}}{V^*_{CC}}.\frac{|I_{ave}|}{I^*_C}.f_{sw}. \tag{12}$$

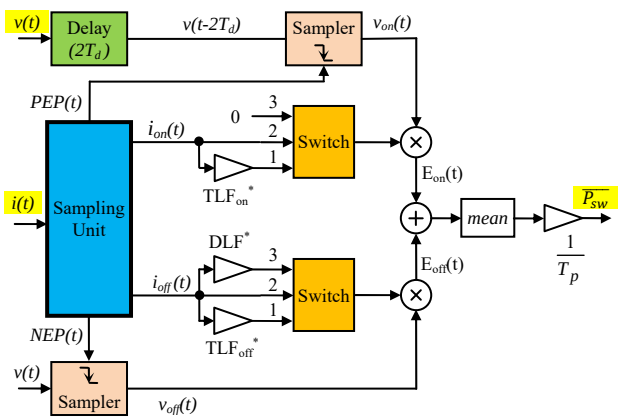

Fig. 1. Block diagram of the proposed method for calculating the average switching power losses in a transistor and its antiparallel diode.

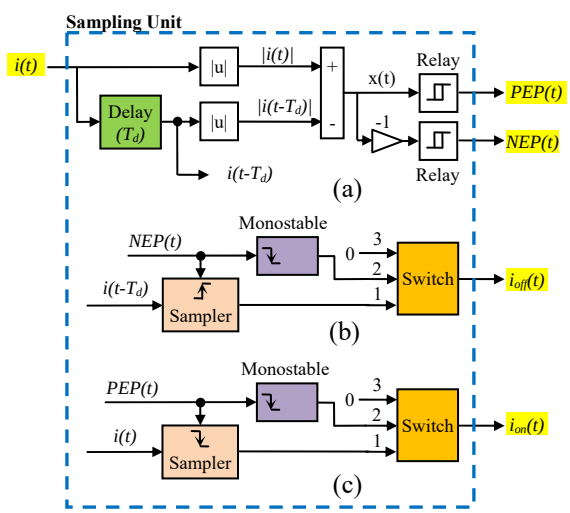

Fig. 2. Details of the "Sampling Unit" block of Fig. 1: (a) generating *PEP(t)* and *NEP(t)*, (b) generating $i_{off}(t)$, and (c) generating $i_{on}(t)$.

In this equation, $V^*_{CC,x}$, $I^*_{C,x}$, and $V_{CC,x}$ are substituted with the constant values of V^*_{CC}, I^*_C, and V_{CC}, respectively.

According to Equ. (12), the average switching power loss of a power switch exhibits a linear relationship with the average amount of its current. This equation is a special case of the proposed method in the current study and will malfunction under the following conditions: 1) when the switching frequency varies during the simulation as in the hysteresis switching technique; 2) when the switching frequency is low, and the switch current varies considerably during the on-state interval of the switch.

In the present study, an appropriate technique based on the switching loss models as Equs. (9) and (10) is proposed to deal with the above-mentioned problems. This method is used to calculate the average value of switching power losses of a transistor and its antiparallel diode, when the switch current or voltage is alternative. Proposed method is described in Fig. 1

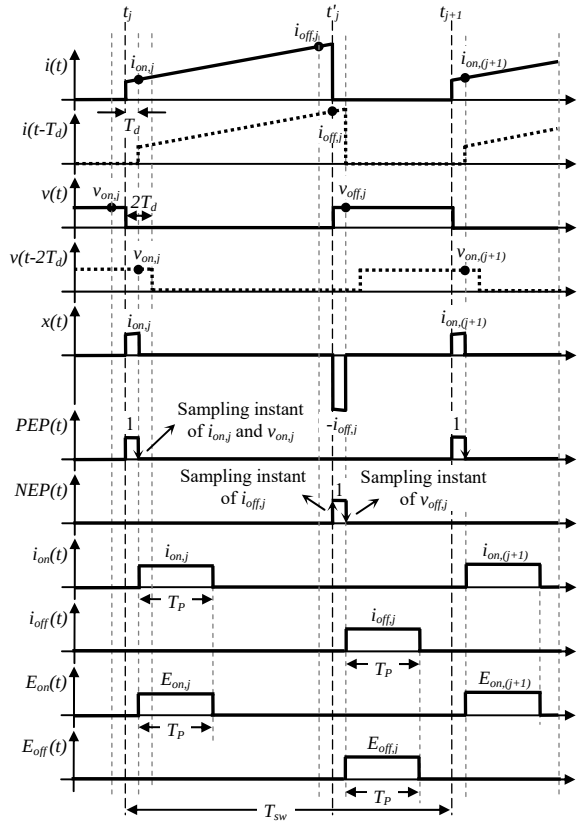

Fig. 3. Generated signals in the proposed method for calculating the average switching power losses in a switch when $i(t) \geq 0$.

and Fig. 2 in the form of a block diagram, and can be implemented easily in simulation environments. Each of the curve fitting equations described in the previous section can be utilized in this method instead of Equs. (9) and (10).

In Fig. 1, the switch current *i(t)* and its voltage *v(t)* are the input variables of the proposed method. The positive value of *i(t)* indicates that the current passes through the transistor whereas the negative value means that the current passes through the antiparallel diode.

If $f_{sw}=1/T_{sw}$ represents the switching frequency, and $f=1/T$ represents the main frequency of the switch current, then $n=T/T_{sw}$ will be the number of the switching operations during a period of the switch current. For the jth switching operation of *n* ones, *i(t)* and *v(t)* along with some other waveforms are shown in Fig. 3. These waveforms are used to describe the operation of the proposed method.

The current and voltage of the switch used in Equs. (9) and (10) are measured shortly before or after turn-on and turn-off transitions, when they have a stable value. As shown in Fig. 3, when the switch is turned on at t_j, the value of the switch current shortly after t_j, $i_{on,j}=i(t_j+T_d)$, is sampled. Moreover, the value of the switch voltage shortly before t_j, $v_{on,j}=v(t_j-T_d)$, is also sampled. Then, these samples are used in Equ. (10) for calculating $E_{sw,on}$.

In addition, when the switch is turned off at t'_j, the value of the switch current shortly before t'_j, $i_{off,j}=i(t'_j-T_d)$, and the value of the switch voltage shortly after t'_j, $v_{off,j}=v(t'_j+T_d)$, are sampled

and used in Equ. (9) for calculating $E_{sw,off}$.

As shown in Fig. 3, the negative and positive edges of control signals *PEP(t)* and *NEP(t)* are used for obtaining $i_{on,j}$, $i_{off,j}$, $v_{on,j}$, and $v_{off,j}$. The signals *i(t)* and $v(t-2T_d)$ are sampled respectively as $i_{on,j}$ and $v_{on,j}$, when the edge of *PEP(t)* is negative. In addition, the signal $i(t-T_d)$ is sampled as $i_{off,j}$ when the edge of *NEP(t)* is positive, and the signal *v(t)* is sampled as $v_{off,j}$ when the edge of *NEP(t)* is negative. The sampler blocks in Fig. 1 and Fig. 2 perform the above-mentioned process using control signals *PEP(t)* and *NEP(t)*.

The generating process of *PEP(t)*, a square pulse at the positive edge of $|i(t)|$, and *NEP(t)*, a square pulse at the negative edge of $|i(t)|$, with the pulse width of T_d is described in Fig. 2(a). In this figure, the "Relay" blocks present a Schmitt trigger characteristic [26] and are described by Equ. (13).

$$PEP(t) = \begin{cases} 1 & x(t) > k_U \\ 0 & x(t) < k_L \end{cases} \quad (13)$$

In the equation above, *x(t)* is the input signal, *PEP(t)* is the output signal, k_U is the lower limit, and k_L is the upper limit of the block. *x(t)*, *PEP(t)*, and *NEP(t)* are shown in Fig. 3.

As shown in Fig. 3, the square pulse $i_{on}(t)$ with the pulse width of T_p and the amplitude of $i_{on,j}$ is generated when the edge of *PEP(t)* is negative. Moreover, the square pulse $i_{off}(t)$ with the pulse width of T_p and the amplitude of $i_{off,j}$ is generated when the edge of *NEP(t)* is negative. The signals $i_{on}(t)$ and $i_{off}(t)$ are generated in Fig. 2(b, c) using "Monostable" [26] and "Switch" blocks. In the Monostable block, one square pulse with pulse width of T_p and amplitude of 1 is generated for each negative edge of input signal. The large value of T_p will improve the accuracy of the proposed method, but its maximum value is limited to T_{sw}. The Switch block in Fig. 2(b, c) is a conditional block and works as follows. For the positive values of the applied signal to input 2, the output of the block is connected to input 3; and for other values, the output is connected to input 1.

In Fig. 1, the Switch blocks are used to distinguish the transistor current from its antiparallel diode current. As mentioned previously, the positive value of $i_{on}(t)$ indicates that the current passes through the transistor. For calculating $E_{sw,on}$ by Equ. (10), $i_{on}(t)$ is multiplied at first by the constant number TLF_{on}^* and then by the switch sampled off-state voltage $v_{on}(t)$. TLF_{on}^* is the transistor turn-on switching loss factor and is defined using Equ. (14). In this equation, V_{CC}^* and I_C^* are constant values that are used respectively instead of $V_{CC,on}^*$ and $I_{C,on}^*$ in Equ. (10). However, the negative amount of $i_{on}(t)$ means that the current passes through the antiparallel diode. As shown in Fig. 1, the turn-on switching loss of the diode is zero because it is usually ignored [4], [9], [10]. The resulted signal from $i_{on}(t)$ is denoted as $E_{on}(t)$ in Fig. 1. Therefore, $E_{on,j}$, the amplitude of jth pulse of $E_{on}(t)$ in Fig. 3, is equal to $TLF_{on}^*.v_{on,j}.i_{on,j}$. In this way, $E_{on,j}$ indicates the turn-on switching energy losses of the switch, for the jth turn-on transition during *T*, a period of the fundamental component of switch current. As mentioned previously, the number of the switching operations during the period *T* is equal to *n*. As a result, the average turn-on switching power loss of the device, $\overline{P_{sw,on}}$, is obtained using Equ. (15). In this equation, function **mean**(*x*) calculates the average value of variable *x* during *T*.

$$TLF_{on}^* = \frac{E_{sw,on}^*}{V_{CC}^*.I_C^*} \quad (14)$$

$$\begin{aligned} \overline{P_{sw,on}} &= \frac{1}{T}\left(E_{on,1} + \ldots E_{on,j} + \ldots E_{on,n}\right) \\ &= \frac{1}{T_p}.\mathbf{mean}\left(E_{on}(t)\right) \end{aligned} \quad (15)$$

As shown in Fig. 1, $E_{off}(t)$ is obtained via multiplying $i_{off}(t)$ by suitable factors, like the method of obtaining $E_{on}(t)$ from $i_{on}(t)$. For calculating $E_{sw,off}$ by Equ. (9), at first, $i_{off}(t)$ is multiplied by TLF_{off}^* when it passes through the transistor, or multiplied by DLF^* when it passes through the antiparallel diode. Next, it is multiplied by switch sampled off-state voltage $v_{off}(t)$. The constants TLF_{off}^* and DLF^*, are the transistor and diode turn-off switching loss factors respectively, and are defined as follows.

$$TLF_{off}^* = \frac{E_{sw,off}^*}{V_{CC}^*.I_C^*}, \quad DLF^* = \frac{-E_{rr}^*}{V_{CC}^*.I_D^*} \quad (16)$$

In this equation, V_{CC}^* and I_C^* are the constant values that are used respectively instead of $V_{CC,off}^*$ and $I_{C,off}^*$ in Equ. (9). Moreover, E_{rr}^* represents the antiparallel diode reverse recovery energy losses, which are measured experimentally during the diode turn-off transition. E_{rr}^* is available in the switch datasheet for the specified V_{CC}^* and I_D^*. V_{CC}^* is the switched off-state voltage of the diode, and I_D^* is its switched on-state current.

Thus, $E_{off,j}$, the amplitude of the jth pulse of $E_{off}(t)$ in Fig. 3, is equal to $TLF_{off}^*.v_{off,j}.i_{off,j}$ or $DLF^*.v_{off,j}.i_{off,j}$. Therefore, $E_{off,j}$ indicates the turn-off switching energy losses of the switch for the jth turn-off transition during the period *T*. As a result, the average turn-off switching power losses of the switch, $\overline{P_{sw,off}}$, can be obtained as follows.

$$\begin{aligned} \overline{P_{sw,off}} &= \frac{1}{T}\left(E_{off,1} + \ldots E_{off,j} + \ldots E_{off,n}\right) \\ &= \frac{1}{T_p}.\mathbf{mean}\left(E_{off}(t)\right) \end{aligned} \quad (17)$$

Using Eques. (15) and (17), the average switching power loss of each switch, $\overline{P_{sw}}$, is calculated by Equ. (18). This equation is implemented in Fig. 1.

$$\overline{P_{sw}} = \overline{P_{sw,on}} + \overline{P_{sw,off}} = \frac{1}{T_p}.\mathbf{mean}\left(E_{on}(t) + E_{off}(t)\right) \quad (18)$$

In Fig. 1, the coefficient $1/T_p$ can be eliminated by modifying the loss factors as Equ. (19). This simplification will reduce the computational burden of the proposed method.

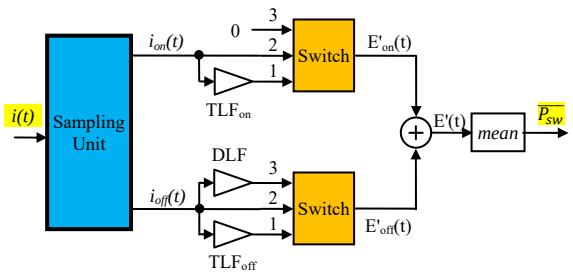

Fig. 4. Simplified block diagram of the proposed method in Fig. 1 when the switch-off state voltage is constant and predefined.

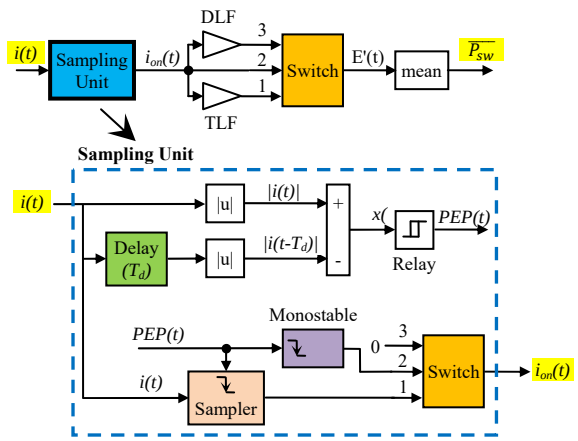

Fig. 5. Simplified block diagram of the proposed method in Fig. 4 when the switching frequency is high.

$$TLF_{on}^{**} = \frac{1}{T_p}.TLF_{on}^{*} \quad , \quad TLF_{off}^{**} = \frac{1}{T_p}.TLF_{off}^{*}$$
$$DLF^{**} = \frac{1}{T_p}.DLF^{*} \tag{19}$$

The switch off-state voltage is usually constant and equal to DC link voltage. Thus, measuring and sampling of this voltage can be eliminated in Fig. 1. In this state, the proposed method in Fig. 1 can be simplified as shown in Fig. 4. TLF_{on}, TLF_{off}, and DLF in Fig. 4 are defined using Equ. (20), which is obtained from Equ. (19). In Equ. (20), V_{CC} is the constant and predefined off-state voltage of the switch.

$$TLF_{on} = \frac{V_{CC}.E_{sw,on}^{*}}{T_p.V_{CC}^{*}.I_C^{*}} \quad , \quad TLF_{off} = \frac{V_{CC}.E_{sw,off}^{*}}{T_p.V_{CC}^{*}.I_C^{*}}$$
$$DLF = -\frac{V_{CC}.E_{rr}^{*}}{T_p.V_{CC}^{*}.I_D^{*}} \tag{20}$$

When the switching frequency is high, switch current cannot change considerably during the time interval that switch is on. Therefore, in this state, the current $i_{on,j}$ in Fig. 3 can be approximately equal to $i_{off,j}$. Therefore, for high switching frequency and specified switch off-state voltage, the proposed method in Fig. 4 can be simplified as shown in Fig. 5. TLF in this figure is defined as follows.

$$TLF = \frac{V_{CC}.(E_{sw,on}^{*} + E_{sw,off}^{*})}{T_p.V_{CC}^{*}.I_C^{*}} \tag{21}$$

III. Calculating Conduction and Total Losses

If the value of rising and falling times of the switch current and voltage are set to be zero, then the switching losses of the switch will also be zero. In this case, the switch losses include only the conduction (on-mode) and off-mode losses. Since the switch losses in the off-mode are negligible in comparison with the conduction losses, the average conduction power losses of the switch $\overline{P_{on}}$ can be calculated as follows.

$$\overline{P_{sw}} = 0 \Rightarrow \overline{P_{on}} \simeq \frac{1}{T}\int_{t_0}^{t_0+T} i(t)\times v(t)\times dt \tag{22}$$

In the equation above, $i(t)$ and $v(t)$ are the current and voltage of the switch, $\overline{P_{sw}}$ denotes the average switching losses, and T is the period of the switch current.

The amount of $\overline{P_{on}}$ is affected significantly by the voltage drop across the switch in the conduction mode. This voltage is affected considerably by the switch current. The accurate value for voltage drop can be calculated by modeling the switch in conduction mode using a DC voltage source and a resistor in series. In this model, the voltage source represents the device threshold voltage V_T, and the resistor indicates the resistance of the switch in the conduction mode R_{on}. This model is used in [15]-[17], [20], and [25] as Equ. (23). In this equation, $v_{on}(t)$ is the forward on-state voltage of the switch.

$$v_{on}(t) = V_T + R_{on}.i(t) \tag{23}$$

By substituting the equation above in Equ. (22), the following equation for calculating $\overline{P_{on}}$ is obtained [25].

$$\overline{P_{on}} = V_T.|I_{ave}| + R_{on}.I_{rms}^2 \tag{24}$$

In the equation above, I_{ave} and I_{rms} are the average and rms value of the switch current $i_C(t)$, respectively.

Other methods are also used in articles as follows. In [5] and [21], $v_{on}(t)$ is represented as Equ. (25) by utilizing curve fitting methods. In this equation, V_0, A, and B are the fitting constants. In [17] and [16], an analytical model is derived for calculating the average conduction losses for some of the converters.

$$v_{on}(t) = V_0 + A.i(t)^B \tag{25}$$

In this study, Equs. (22) and (23) are used to calculate the average conduction losses.

A. Average Total Power Loss

The calculation of $\overline{P_{sw}}$ and $\overline{P_{on}}$ was described in the previous sections. By utilizing them, the average total power losses of the semiconductor switch, $\overline{P_{tot}}$, is calculated as follows.

$$\overline{P_{tot}} = \overline{P_{sw}} + \overline{P_{on}} + \overline{P_{off}} \simeq \overline{P_{sw}} + \overline{P_{on}} \tag{26}$$

The congruence of the calculated power losses with the experimental results is attributed to the accuracy of the parameter values of the switch loss model. The parameters of a switch which are used in the selected switch loss models are summarized in Table II. This table includes the parameter

TABLE II
PARAMETERS OF SOME IGBTS AT THE HIGH JUNCTION TEMPERATURE; THESE PARAMETERS ARE REQUIRED FOR COMPUTING SWITCH LOSSES
(V_n=600 V, V_{cc}^*=300 V, I_C^*= I_D^*= I_n)

Name	Part Num.	I_n (A)	Transistor (IGBT)			Antiparallel diode		
			E_{on}^*, E_{off}^* (mj)	V_T (v)	R_{on} mΩ	V_T (v)	R_{on} mΩ	E_{rr}^* (mj)
S1	SKiiP 28GH066V1	100	3.4, 3.5	1	9	0.9	6	3.3
S2	SK50GBB0 66ET	50	2.2, 1.7	0.8	17	0.9	12	0.7
S3	2MBI100V A-060-50	100	5, 4	0.8	12	0.8	6	2.1

values of some IGBTs when the junction temperature is high. These parameters are easily obtained via the datasheets. Switches S1 and S2 of this table are produced by the SEMIKRON company, and switch S3 is produced by the FUJI ELECTRIC company.

B. Dependency of Switch Losses on the Junction Temperature

The methods for calculating the conduction and switching losses of the power switches can be classified into two categories: 1) the methods that consider the dependency of the switch characteristic on the junction temperature, and 2) the methods that ignore such assumptions and use the constant characteristics of the switches obtained for the maximum junction temperature. The second methods can be implemented readily. However, the first methods are computationally demanding and can calculate the losses more accurately.

In [27], a five-step iterative process is used to consider the junction temperature effects on the switching losses. In [16], only the conduction losses of the switch are related to the junction temperature. The dependency of the losses on the temperature is investigated extensively in [20] by relating the conduction and also switching losses to the temperature.

In [20], the losses of the semiconductor switches are increased by only 10% through increasing the heat sink temperature from 30 °C to 100 °C. This result shows that the parameters of the power switch can be obtained for the maximum junction temperature and can be used to calculate the losses as in [6]. Therefore, this method is acceptable because the error in the calculated losses is within the acceptable range when the temperature effect on the losses is neglected. Moreover, a converter which is designed for the worst conditions (switch parameters in the maximum junction temperature), will also operate correctly for other allowed conditions (switch parameters in the lower junction temperatures).

IV. SIMULATION RESULTS

The proposed method for calculating the average switching and conduction power losses of a power switch, is implemented

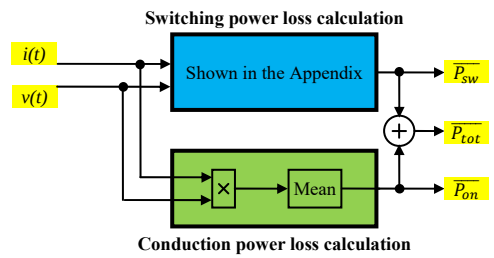

Fig. 6. Proposed method in the MATLAB/SIMULINK environment for calculating the average losses of a power switch.

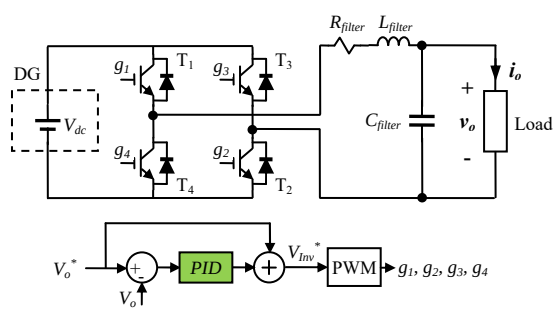

Fig. 7. Single-phase voltage source inverter used for connecting a DC source to the AC load.

TABLE III
CHARACTERISTICS OF THE SINGLE-PHASE INVERTER WITH THE NOMINAL CURRENT OF 50 A

Parameter	Value	Parameter	Value
V_o^*	220 V(rms)/50 Hz	V_{dc}	544 V
P_{Load}, Q_{Load}	7.5 kW, 5.6 kVAR	PID controller	P = 18
R_{filter}, L_{filter}	2.6 mΩ, 2.6 mH		I = 5400
C_{filter}	100 μF		D = 0.001
			N = 30000

in the MATLAB/SIMULINK software as shown in Fig. 6. The "switching power loss calculation" block of this figure is described in Fig. 1 and is implemented in the SIMULINK environment as shown in the appendix (Fig. 15). Moreover, the "conduction power loss calculation" block of Fig. 6 operates based on Equ. (22). Equ. (23) is implemented in the IGBT model for generating the switch on-state voltage $v_{on}(t)$.

A. Evaluating the Operation of the Proposed Method

For evaluating the performance of the proposed method, this method is used to calculate the average power losses of a single-phase inverter. As shown in Fig. 7, the inverter is composed of an H-bridge and an LC filter and is used to connect a DC source to the AC load. The characteristics of the inverter and the load are summarized in Table III.

Considering the amount of 50 kHz for the upper limit of the switching frequency, the maximum value of T_p will be equal to 20 μs in simulations. The duration of the voltage or current oscillations after switching is one of the parameters that affect the value of T_d. For the simulations in this study, T_d is set to 2 μs.

As shown in Fig. 8, each square pulse of $i_{on}(t)$ is generated at

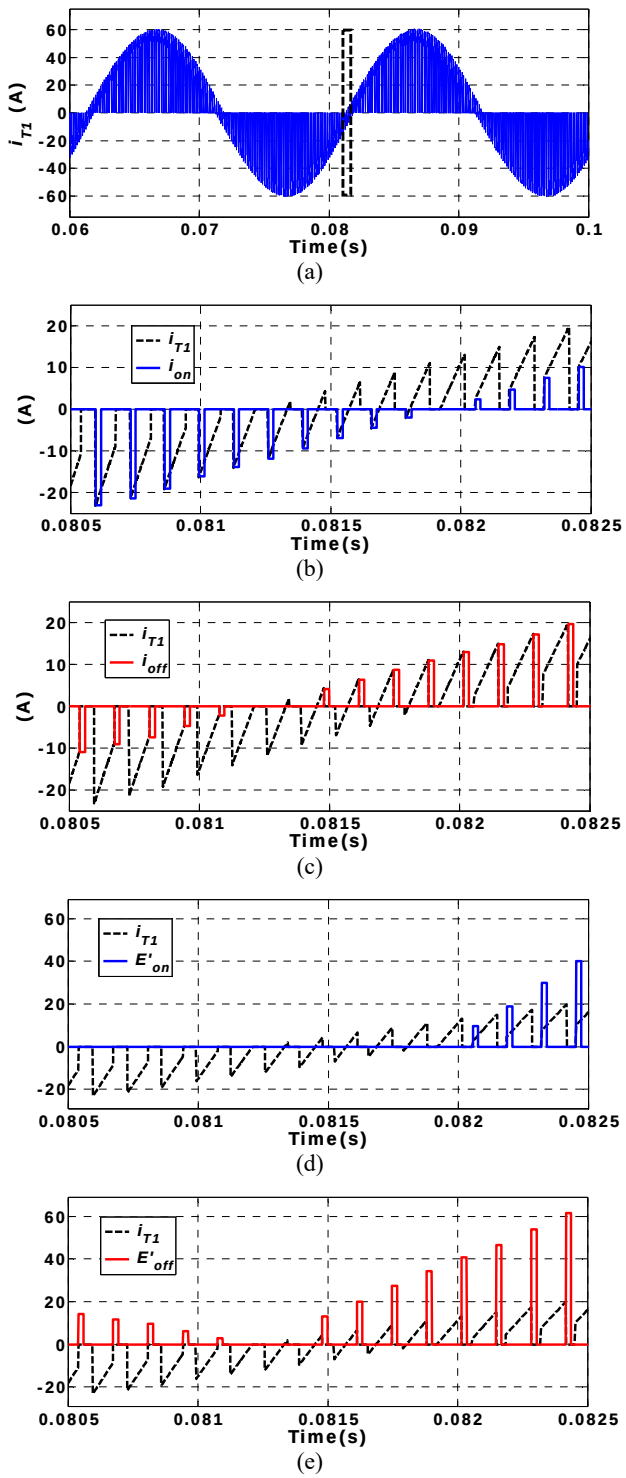

Fig. 8. Number of waveforms in the proposed method in Fig. 4 that are used for calculating the average switching loss of switch T_1 in Fig. 7: (a) switch current (i_{T1}), (b) i_{T1} and square current at turn-on time (i_{on}), (c) i_{T1} and square current at turn-off time (i_{off}), (d) i_{T1} and square switching loss at turn-on time (E'_{on}), and (e) i_{T1} and square switching loss at turn-off time (E'_{off}).

the moment that the switch is turned on as described previously in Fig. 3. As shown, each pulse is generated with the pulse width of T_p and with the amplitude that is equal to the switch current shortly after the turn-on transition.

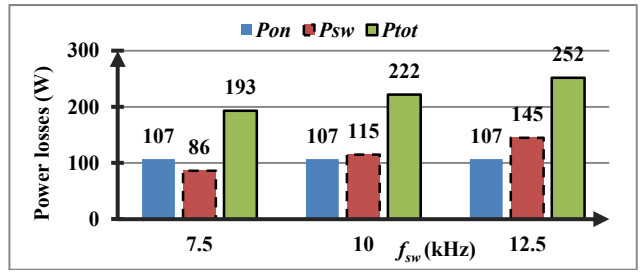

Fig. 9. Power losses of the described inverter in Table III when constructed by switch S2 for some switching frequencies.

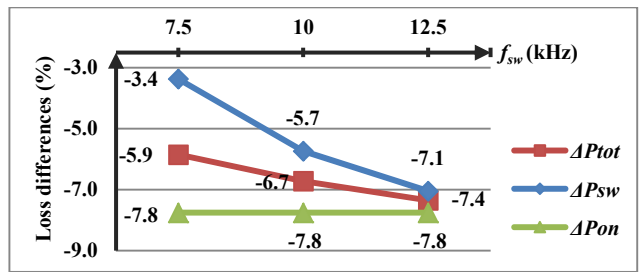

Fig. 10. Relative differences between the losses obtained by the proposed method and the Semisel software versus some switching frequencies f_{sw}.

The signal $i_{off}(t)$ in Fig. 8 is similar to that in Fig. 3. In other words, each square pulse of $i_{off}(t)$ is generated at the turn-off moment of the switch. Furthermore, the duration of each pulse is equal to T_p, and its amplitude is equal to the switch current shortly before the turn-off transition.

In Fig. 7, the off-state voltage of the switches is constant and is equal to V_{dc}. Therefore, the simplified form of the proposed method in Fig. 4 is used to calculate the switching power losses.

Switch S2 in Table II is suitable for constructing the intended inverter with the nominal current of 50 A. Using the V_{dc} from Table III and characteristics of S2, the amount of the loss factors TLF_{on}, TLF_{off}, and DLF in Fig. 4 are obtained by Equ. (20) as: $TLF_{on} \simeq 3.9893$, $TLF_{off} \simeq 3.1371$, and $DLF \simeq -1.3056$.

Using the adjusted proposed method, the losses of the inverter are calculated and shown in Fig. 9. In this figure, *Pon*, *Psw*, and *Ptot* are the average amount of the conduction, switching, and total power losses of the inverter, respectively.

B. Evaluating the Accuracy of the Calculated Losses

1) Using the IGBT Loss Simulator Programs: The accuracy of the calculated losses can be evaluated by comparing them with the losses obtained via loss simulator programs under the same conditions. These programs are provided by the manufacturers of power electronics devices. For example, Semisel-Simulation Software V4.1.2 [11] and FUJI IGBT Simulator V6 [12] are two loss simulator programs presented by the SEMIKRON and FUJI ELECTRIC companies, respectively. These programs can calculate the losses of the single-phase and three-phase inverters designed by the transistors of the associated companies.

For the described inverter in Table III, the relative differences between the losses obtained by the proposed method and Semisel software are calculated by Equ. (27). The results of

TABLE IV
CHARACTERISTICS OF THE SINGLE-PHASE INVERTER WITH THE NOMINAL CURRENT OF 100 A

Parameter	Value	Parameter	Value
V_o^*	220 V(rms)/50 Hz	V_{dc}	400 V
P_{Load}, Q_{Load}	12.5 kW, 9.3 kVAR	PID controller	$\boldsymbol{P}$ = 14 $\boldsymbol{I}$ = 8700 $\boldsymbol{D}$ = 0.001 $\boldsymbol{N}$ = 43000
R_{filter}, L_{filter}	1 mΩ, 1 mH		
C_{filter}	100 µF		

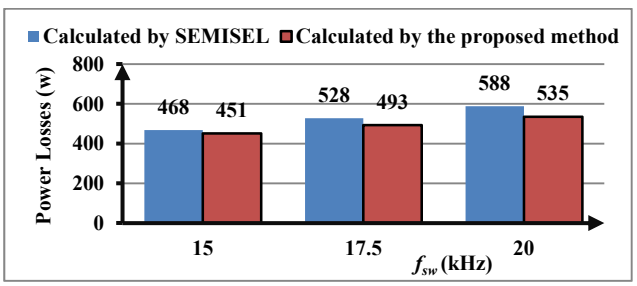

(a) Designed by S1.

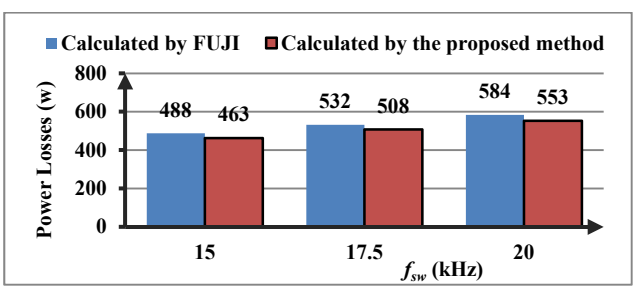

(b) Designed by S3.

Fig. 11. Total power losses of the described inverter in Table IV for some switching frequencies.

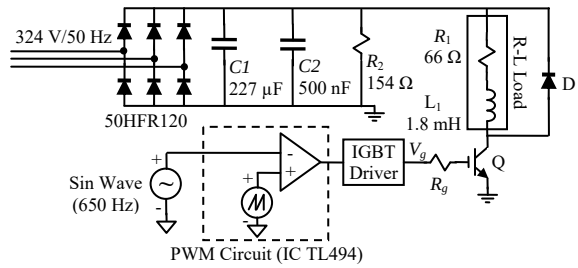

(a)

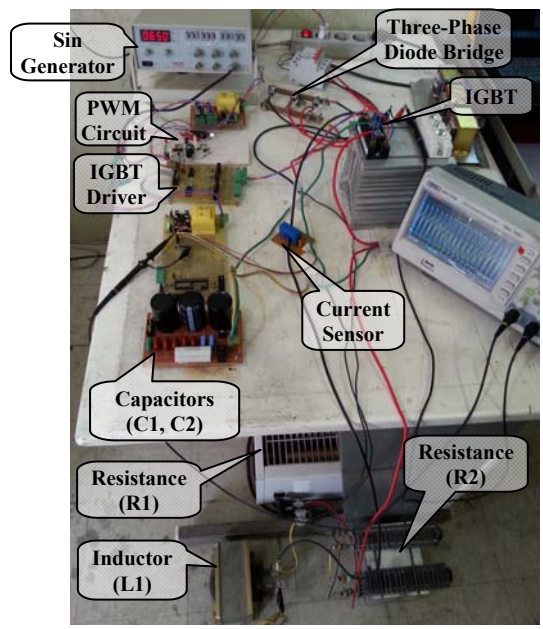

(b)

Fig. 12. A proper electrical circuit for evaluating the proposed method experimentally (a) and its laboratory prototype (b).

these calculations for some switching frequencies are shown in Fig. 10. As discussed in part B of Section III, the comparison is conducted under the worst conditions. In other words, the parameter values of S2 in Table II are obtained at the high temperature. In addition, the thermal parameters in the Semisel software are adjusted properly to ensure that the junction temperature to be high.

$$\Delta Ptot = 100 \times \frac{Ptot_{Proposed\ method} - Ptot_{Semisel}}{Ptot_{Semisel}} \tag{27}$$

In the equation above, *Ptot* is the average total power loss of the inverter. This parameter can be substituted by the switching power loss *Psw* and conduction power loss *Pon* to obtain *ΔPsw* and *ΔPon*, respectively. As shown in Fig. 10, the power losses obtained by the proposed method are slightly smaller than the losses obtained by the Semisel software; however, the differences are acceptable.

The characteristics of the intended inverter are changed as shown in Table IV. Switches S1 and S3 in Table II are suitable for constructing this new inverter with the nominal current of 100 A. The average power losses of this inverter are shown in Fig. 11 versus some switching frequencies for two designs: 1) the inverter by SEMIKRON IGBT (S1) and 2) the inverter by FUJI IGBT (S3). For these designs, the inverter losses in the worst conditions are calculated by two methods: 1) the proposed method in this study and 2) the associated loss simulation software tools (Semisel-Simulation and FUJI IGBT Simulator). As shown in Fig. 11, the power losses calculated by the proposed method show an acceptable congruence with the power losses obtained by the associated loss simulator software.

2) Using the Experimental Results: The accuracy of the proposed method can also be evaluated using the experimental results. Thus, the proposed electrical circuit in Fig. 12(a) was constructed and used to obtain the experimental data. The constructed laboratory prototype is shown in Fig. 12(b). As shown in Fig. 12(a), the switched voltage is provided by a three-phase diode bridge rectifier. Therefore, the switched voltage remains approximately constant over time with the value of 550 V as shown in Fig. 13(a).

The alternative load current in Fig. 12(a) will cause the switched current to become alternative. Therefore, an alternative current with the frequency of 650 Hz flows in the R-L load as shown in Fig. 13(a). This current is generated using

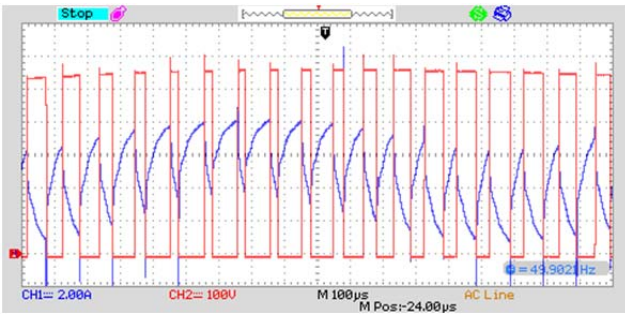

(a)

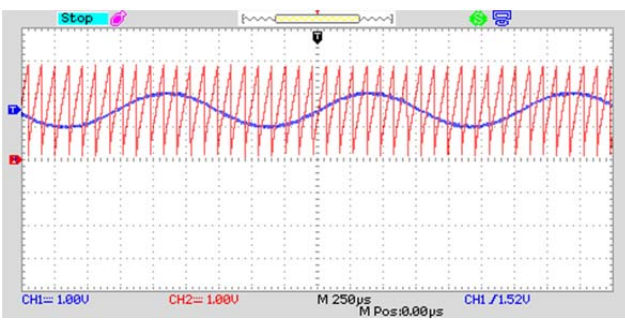

(b)

Fig. 13. Waveforms obtained from the laboratory prototype: (a) the IGBT voltage (square waveform) and load current, and (b) triangular and sinusoidal waveforms used for generating alternative switched current by PWM.

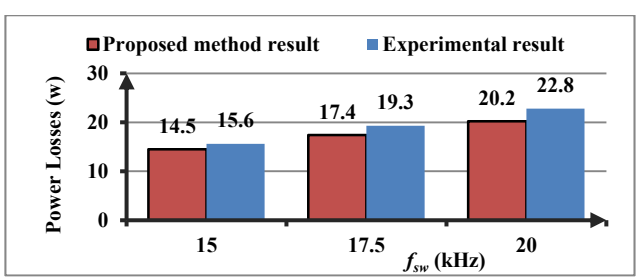

Fig. 14. Average total power losses of the IGBT of the constructed laboratory prototype for some switching frequencies.

TABLE V
MEASURED PARAMETERS OF THE IGBT USED IN LABORATORY PROTOTYPE FOR THE LOW JUNCTION TEMPERATURE
(V_n= 1200 V, I_n= 75 A, V_{cc}^*= 600 V, I_C^*= I_D^*= I_n)

Part Num.	Transistor (IGBT)			Antiparallel diode		
	E_{on}^*, E_{off}^* (mj)	V_T (v)	R_{on} mΩ	V_T (v)	R_{on} mΩ	E_{rr}^* (mj)
SKM75GB12T4	2.6, 15.5	0.8	17.4	0.96	21	4.3

the pulse-width modulation (PWM) technique as shown in Fig 12(a). The triangular and sinusoidal waveforms used in the PWM technique are shown in Fig. 13(b). An oscilloscope (GPS 1072B) with the memory length of 20480 points, and sample rate of 12.5 MSa/s was used to measure and save the switched voltage and current waveforms. Considering the limited memory length, the frequency of load current should be increased to 650 Hz to decrease its period time and making it possible to gather all the current samples in one period.

The measured and saved waveforms of the switch voltage and current are used to measure the total power losses of the switch. The used switch is an IGBT from the products of the SEMIKRON company. The average power losses of the transistor of the constructed prototype, were measured for some switching frequencies and are demonstrated in Fig. 14.

The parameters of the loss models of the IGBT used in prototype are summarized in Table V. The values of the parameters have been measured in the laboratory for the low junction temperature and the characteristics of the used IGBT driver (V_g = ± 15 V, and R_g = 10 Ω). These values are used in the proposed method, and the average total power losses of the IGBT of the laboratory prototype are calculated in the simulation environment. The calculated losses and the measured losses are shown in Fig. 14, for some switching frequencies. As shown, the calculated losses present an acceptable congruence with the measured losses. Therefore, the proposed method is operating correctly.

V. CONCLUSION

In this study, switching loss calculation models are comprehensively reviewed for the first time. Accordingly, a proper loss model with the less computational burden is selected. The study mainly contributes by establishing an applicable technique with details for obtaining the average switching power loss by utilizing selected switching loss model. This technique works properly when switched current or switched voltage is alternative. In addition, the technique can be implemented easily using the basic blocks of programs such as MATLAB/SIMULINK. Furthermore, the switched voltage and switched current are sampled properly in the proposed method.

The performance of the proposed method is evaluated by the simulation and experimental results. In the simulation environment, the proposed method is used to obtain the average switching power losses of a single-phase inverter. For various types of IGBTs, the inverter losses are calculated using the proposed method and compared with losses obtained by the loss simulator tools. The similar values of the compared losses confirm the accuracy of the proposed method.

APPENDIX

An implementation of Fig. 1 in the MATLAB/SIMULINK software environment is shown in details in Fig. 15.

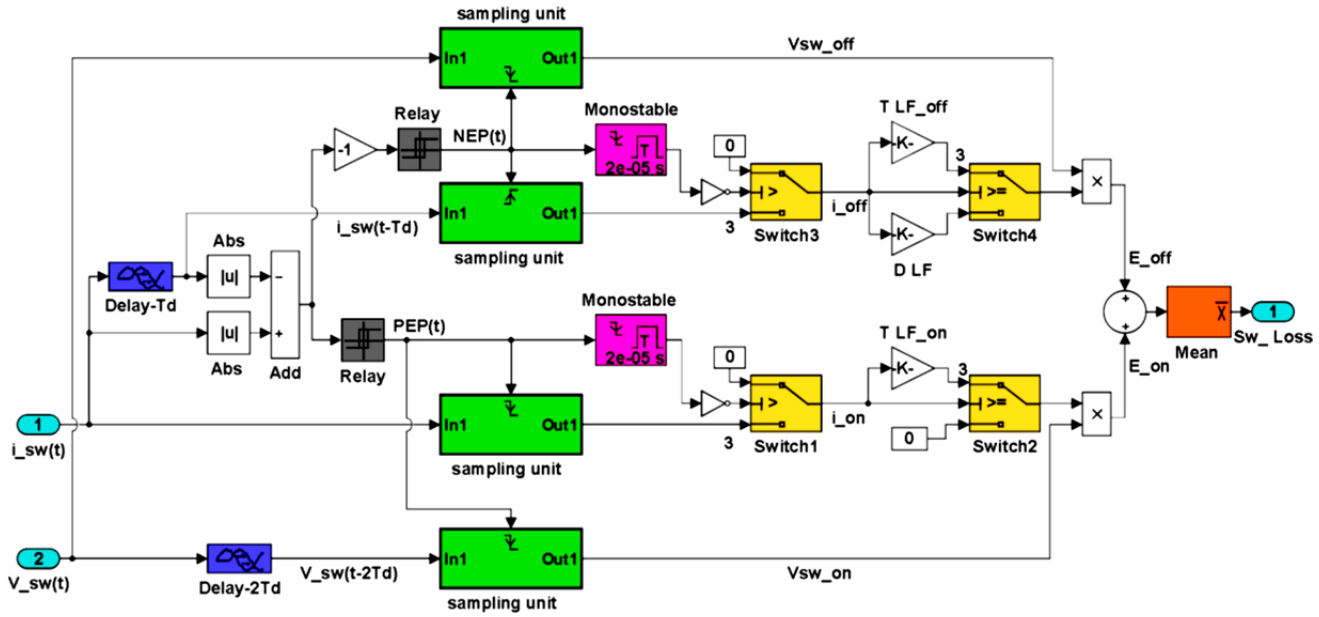

Fig. 15. Implementation of the proposed method in the MATLAB/SIMULINK software environment.

REFERENCES

[1] L. Xiaonan, J. M. Guerrero, S. Kai, J. C. Vasquez, R. Teodorescu, and H. Lipei, "Hierarchical control of parallel AC-DC converter interfaces for hybrid microgrids," *IEEE Trans. Smart Grid,* Vol. 5, No. 2, pp. 683-692, Mar. 2014.

[2] T. Xin, K. M. Tsang, and W. L. Chan, "A power quality compensator with DG interface capability using repetitive control," *IEEE Trans. Energy Convers.,* Vol. 27, No. 2, pp. 213-219, Jun. 2012.

[3] M. H. Rashid, *Power Electronics: Circuits, Devices & Applications*, 4th ed.: Prentice Hall, 2013.

[4] Y. Suh, J. K. Steinke, and P. K. Steimer, "Efficiency comparison of voltage-source and current-source drive systems for medium-voltage applications," *IEEE Trans. Ind. Electron.,* Vol. 54, No. 5, pp. 2521-2531, Oct. 2007.

[5] D. Krug, S. Bernet, S. S. Fazel, K. Jalili, and M. Malinowski, "Comparison of 2.3-kV medium-voltage multilevel converters for industrial medium-voltage drives," *IEEE Trans. Ind. Electron.,* Vol. 54, No. 6, pp. 2979-2992, Dec. 2007.

[6] S. Bernet, S. Ponnaluri, and R. Teichmann, "Design and loss comparison of matrix converters and voltage-source converters for modern AC drives," *IEEE Trans. Ind. Electron.,* Vol. 49, No. 2, pp. 304-314, Apr. 2002.

[7] D. Barater, E. Lorenzani, C. Concari, G. Franceschini, and G. Buticchi, "Recent advances in single-phase transformerless photovoltaic inverters," *IET Renewable Power Generation,* Vol. 10, No. 2, pp. 260-273, Feb. 2016.

[8] M. Liang, T. Q. Zheng, and Y. Li, "An improved analytical model for predicting the switching performance of SiC MOSFETs," *Journal of Power Electronics,* Vol. 16, No. 1, pp. 374-387, Jan. 2016.

[9] T. Bruckner and s. Bernet, "Estimation and measurement of junction temperatures in a three-level voltage source converter," *IEEE Trans. Power Electron.,* Vol. 22, No. 1, pp. 3-12, Jan. 2007.

[10] K. You and M. F. Rahman, "Analytical model of conduction and switching losses of matrix-z-source converter," *Journal of Power Electronics,* Vol. 9, No. 2, pp. 275-287, Mar. 2009.

[11] SEMIKRON, *Semisel - Simulation Software, Version 4.1.2*, https://www.semikron.com/service-support/semisel-simulation.html, 2016.

[12] Fuji-Electric, *Fuji IGBT Simulator, Version 6*, http://www.fujielectric.com/products/semiconductor/model/igbt/simulation/index.html, 2016.

[13] F. Schafmeister, S. Herold, and J. W. Kolar, "Evaluation of 1200V-Si-IGBTs and 1300V-SiC-JFETs for application in three-phase very sparse matrix AC-AC converter systems," in *Applied Power Electronics Conference and Exposition (APEC)*, pp. 241-255, 2003.

[14] F. Schafmeister, C. Rytz, and J. W. Kolar, "Analytical calculation of the conduction and switching losses of the conventional matrix converter and the (very) sparse matrix converter," in *Applied Power Electronics Conference and Exposition (APEC)*, pp. 875-881, 2005.

[15] Z. Zhang, Z. Xu, and Y. Xue, "Valve losses evaluation based on piecewise analytical method for MMC–HVDC links," *IEEE Trans. Power Del.,* Vol. 29, No. 3, pp. 1354-1362, Jun. 2014.

[16] H. Wang, G. Tang, Z. He, and J. Cao, "Power loss and junction temperature analysis in the modular multilevel converters for hvdc transmission systems," *Journal of Power Electronics,* Vol. 15, No. 3, pp. 685-694, May 2015.

[17] S. Dieckerhoff, S. Bernet, and D. Krug, "Power loss-oriented evaluation of high voltage igbts and multilevel converters in transformerless traction applications," *IEEE Trans. Power Electron.,* Vol. 20, No. 6, pp. 1328-1336, Nov. 2005.

[18] A. Lopez, D. Patino, and R. Diez, "Efficiency analysis of a ladder multilevel converter with the use of the equivalent continuous model," Vol. 14, No. 6, pp. 1130-1138, Nov. 2014.

[19] R. W. Erickson and D. Maksimovic, *Fundamentals of power electronics*, 2nd ed. New York, Boston, Dordrecht, London, Moscow: Kluwer Academic Publishers, 2004.

[20] Q. Tu and Z. Xu, "Power losses evaluation for modular multilevel converter with junction temperature feedback," in *Proceedings of IEEE Power and Energy Society General Meeting*, pp. 1-7, 2011.
[21] F. Blaabjerg, U. Jaeger, S. Munk-Nielsen, and J. K. Pedersen, "Power losses in PWM-VSI inverter using NPT or PT IGBT devices," *IEEE Trans. Power Electron.,* Vol. 10, No. 3, pp. 358-367, May 1995.
[22] T. Matsuoa, S. Berneta, R. S. Colbyb, and T. A. Lipoa, "Modeling and simulation of matrix converter/induction motor drive," *ELSEVIER Mathematics and Computers in Simulation,* Vol. 46, No. 3, pp. 175-195, May 1998.
[23] B. J. Masserant and T. A. Stuart, "Experimental verification of calculated IGBT losses in PFCs," *IEEE Trans. Aerosp. Electron. Syst.,* Vol. 32, No. 3, pp. 1154-1158, Jul. 1996.
[24] F. Martin, *Semikron innovation+service*, 1st ed.: Semikron International, 2000.
[25] K. Lee, Y. Suh, and Y. Kang, "Loss analysis and comparison of high power semiconductor devices in 5MW PMSG MV wind turbine systems," *Journal of Power Electronics,* Vol. 15, No. 6, pp. 1380-1391, Sep. 2015.
[26] D. A. Bell, *Solid State Pulse Circuits*, 4th ed. USA: Oxford University Press, 2007.
[27] H. A. Mantooth and A. R. Hefner, "Electrothermal simulation of an IGBT PWM inverter," *IEEE Trans. Power Electron.,* Vol. 12, No. 3, pp. 474-484, May 1997.

Seyyed Abbas Saremi Hasari received the B.Sc. degree from Zanjan University, Zanjan, Iran, in 2001 and the M.Sc. degree from Iran University of Science and Technology, Tehran, Iran in 2004, all in Electrical Engineering. He is currently working toward the Ph.D. degree in Shahid Beheshti University, Tehran, Iran. He joined the Department of Electrical Engineering, Islamic Azad university of Karaj Branch, Karaj, Iran, in 2007. His research interests include distributed generation, distribution networks, and applications of power electronics in microgrids.

Ahmad Salemnia received the B.Sc. and M.Sc. degrees from Iran University of Science and Technology, Tehran, Iran, in 1983 and 1990, respectively, and the Ph.D. degree from Polytechnic Institute of Lorraine (INPL), France, in 1996, all in Electrical Engineering. He joined Shahid Abbaspour School of Engineering, Shahid Beheshti University, Tehran, Iran, in 1990, where he is currently an Assistant Professor. His research interests include power quality, harmonics and active filtering, and applications of power electronics in power systems.

Mohsen Hamzeh received the B.Sc. and M.Sc. degrees from University of Tehran, Tehran, Iran, in 2006 and 2008, respectively, and the Ph.D. degree from Sharif University of Technology, Tehran, Iran, in 2012, all in Electrical Engineering. He joined the Department of Electrical Engineering, Shahid Beheshti University, Tehran, Iran, in 2013, where he is currently an Assistant Professor. His research interests include distributed generation, microgrid control, and applications of power electronics in power distribution systems.